

Interpretable AI-Based Prediction of Elastic Modulus in Bamboo-Reinforced Polypropylene Using Mori–Tanaka and Neural Networks

Sameh Fuqaha, Guntur Nugroho and Ahmad Zaki*

Department of Civil Engineering, Universitas Muhammadiyah Yogyakarta, Yogyakarta, Indonesia

ARTICLE INFO

Article history:

Received June 9, 2025

Revised July 23, 2025

Accepted August 12, 2025

Available online September 01, 2025

Keywords:

Bio-composites

Bamboo fiber

Polypropylene

Artificial neural network

Elastic modulus

ABSTRACT

This study presents a hybrid and interpretable modeling framework that integrates the Mori–Tanaka micromechanical model with artificial neural networks (ANNs) to predict the elastic modulus of bamboo-reinforced polypropylene composites. A synthetic dataset was created encompassing bamboo fiber volume fractions from 5% to 25%, enabling the ANN to generalize proficiently across diverse reinforcement setups. The ideal network architecture (2–15–1) attained superior predictive performance, with mean squared errors under 20 and regression coefficients surpassing 0.98, so validating the model's accuracy and robustness. To guarantee reliability, the model was evaluated on intermediate components not encountered during training, exhibiting consistent performance and resilience to overfitting. The interpretability of the black-box AI model was improved via sensitivity analysis and SHAP (Shapley Additive Explanations), which revealed that bamboo modulus was the primary factor affecting composite stiffness, contributing around 72% of predictive influence, whereas polypropylene accounted for 28%. These findings correspond with micromechanical theory and offer insights into material design methodologies. Combining physics-based modeling with artificial intelligence improves the accuracy of predictions and helps engineers make smart choices during the early stages of bio-composite development. This research enhances sustainable material innovation by offering a transparent, efficient, and scalable modeling tool suitable for comprehensive mechanical property forecasts and practical composite design.

1. Introduction

The rising demand for sustainable and eco-friendly materials has generated significant interest in bio-composites, especially in engineering and industrial applications. Bio-composites, consisting of natural fibers integrated into polymer matrices, provide an appealing equilibrium of performance, little environmental impact, and cost [1-3]. Their application is proliferating across sectors like automotive [4,5], construction [6], packaging [7], and electronics [8], attributable to their

biodegradability, lightweight nature, and mechanical strength [9,10].

Bio-composites, derived from renewable resources, enhance sustainability by diminishing dependence on petroleum-based materials and lowering plastic waste, therefore lessening their environmental impact [11,12], [13]. A primary advantage is biodegradability, which simplifies end-of-life waste management by composting and natural deterioration, hence augmenting their environmental appeal [13], [14]. Natural fibers, including flax, hemp, kenaf,

* Corresponding author.

E-mail address: ahmad.zaki@umy.ac.id

DOI: [10.24237/djes.2025.18307](https://doi.org/10.24237/djes.2025.18307)

This work is licensed under a [Creative Commons Attribution 4.0 International License](https://creativecommons.org/licenses/by/4.0/).



and sisal, are markedly lighter than traditional reinforcements such as glass or nylon, facilitating substantial weight reduction in composite structures [15,16]. Flax fibers possess a density of roughly 1.4 g/cm^3 , in contrast to glass fibers, which exhibit a density of about 2.5 g/cm^3 [17]. The rigidity of natural fibers such as flax varies from 50 to 100 GPa, comparable to that of glass fiber [6].

The lightweight characteristics of bio-composites render them exceptionally appropriate for automotive and aeronautical applications, where weight reduction is essential for fuel efficiency and operational performance [15], [18]. Besides weight reduction, bio-composites have a superior strength-to-weight ratio, rendering them mechanically competitive with conventional materials. Their mechanical properties, including as tensile, compressive, and flexural strength, can be optimized through the meticulous selection of natural fibers and biopolymers [19]. Moreover, advancements in fiber treatment methods have enhanced fiber matrix adherence and diminished moisture absorption, hence resolving persistent durability issues in bio-composite applications [20,21].

Bamboo has emerged as a viable reinforcement material among natural fibers due to its high growth rate, recyclability, and superior mechanical qualities [22,23]. The features of bamboo fibers, along with their low cost and wide availability, render them very ideal for strengthening polymer matrices like polypropylene (PP) [23]. Polypropylene is a commonly employed thermoplastic due to its thermal stability, chemical resilience, and compatibility with bio-fillers [24]. The amalgamation of bamboo with polypropylene yields bio-composites that may demonstrate enhanced mechanical properties relative to pure polymers [25]. The incorporation of bamboo particles and ultrafine bamboo-char (UFBC) into polypropylene (PP) markedly improves its tensile strength and modulus. A bio-composite with a 70/25/5 ratio of PP, Bamboo, and UFBC attained a tensile strength of 30.59 MPa, representing a 30% enhancement compared to pure PP. The tensile modulus attained 460.13 MPa, representing a 109% increase compared to pristine PP [26].

Comprehending the mechanical properties of these bio-composites, especially their elastic attributes, is essential for material selection and structural design [27]. Historically, these qualities have been assessed by experimental testing, finite element analysis (FEA), and micromechanical homogenization methods. The Mori-Tanaka homogenization model is a prevalent mean-field method for forecasting the effective properties of heterogeneous materials, especially composites. This approach is predicated on the concept of inclusions within a matrix and employs Eshelby's solution for the inclusion problem, rendering it especially effective for isotropic matrices [28]. Although these methods provide significant insights, they may be time-intensive, computationally intensive, and susceptible to modeling assumptions [29,30]. Advancements in computational tools have enabled artificial intelligence (AI) to effectively model complicated material behavior in materials science. Machine learning methodologies, especially artificial neural networks (ANNs), have exhibited significant capability in identifying non-linear correlations between input variables and mechanical responses [31]. These models derive insights from numerical or experimental datasets and may swiftly forecast material behavior with considerable precision, providing substantial benefits compared to traditional methods.

The utilization of artificial neural networks for the mechanical characterisation of bio-composites has garnered attention in academic literature. Ramful and Casseem [32] created a deep learning model to forecast the mechanical performance of construction-grade bamboo, attaining significant predictive accuracy with a dataset that encompassed its physical attributes. In a separate investigation, Nasri and Toubal [33] utilized ANN models to replicate the behavior of PP composites reinforced with flax and pine fibers, achieving prediction errors between 3% and 6% of experimental values. Saada et al. [34] combined artificial neural networks with response surface methods to forecast tensile characteristics of palm-fiber epoxy composites, achieving R^2 values exceeding 0.97 for both stress and modulus.

Furthermore, Al-Jarrah and AL-Oqla [35] developed a two-stage ANN framework for the categorization of natural fibers according to their chemical composition, achieving a classification accuracy of 95.6%.

This study examines the application of a feed-forward backpropagation neural network to estimate the elastic modulus of polypropylene reinforced with 15% bamboo fiber. The training dataset is artificially created using the Mori–Tanaka micromechanical model, allowing the ANN to comprehend the fundamental structure–property correlations. Our objective is to assess the prediction efficacy of the ANN and illustrate its value as a rapid, precise, and comprehensible instrument in the evaluation of bio-composites. This study enhances the existing literature on sustainable material creation by presenting a hybrid modeling framework that integrates theoretical micromechanics with intelligent

prediction systems. This technique facilitates the shift towards environmentally sustainable, data-driven material design methodologies.

2. Methodology

Figure 1 shows the approach used in this work, which includes all the steps from preparing the materials to creating the computer model. The first step in making the bio-composite is to choose and mix polypropylene (PP) and bamboo fibers. After the material is made, the mechanical properties of each part are measured and used to generate a dataset. The Mori–Tanaka homogenization approach, a micromechanical model that calculates the composite's overall elastic modulus by taking into account how the matrix and the reinforcement work together, was used to produce this dataset.

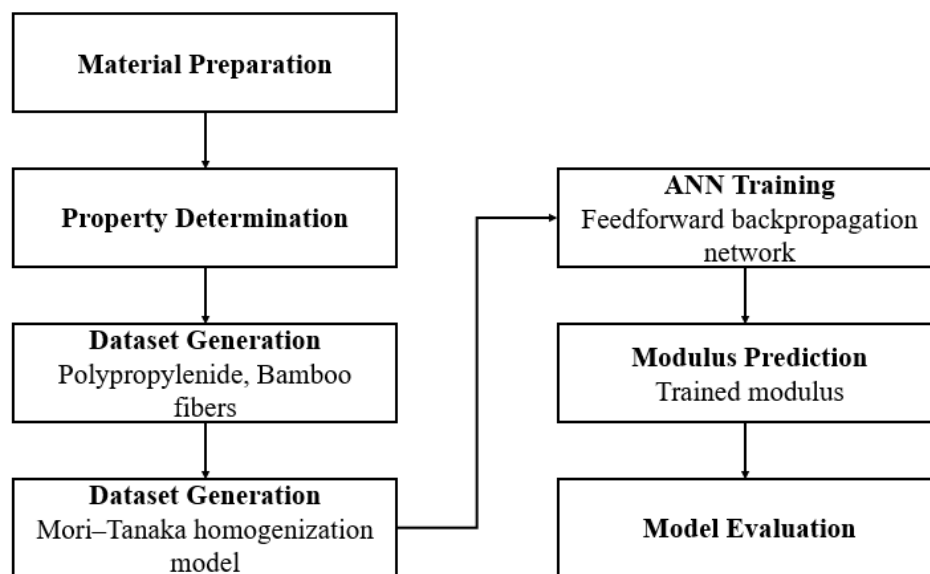


Figure 1. Flowchart illustrates the methodology for predicting the elastic modulus of a polypropylene-bamboo bio-composite.

The artificial neural network (ANN) model created in this study was only trained on synthetic data produced by the Mori–Tanaka micromechanical model. The predictive capability of the ANN is intricately linked to the assumptions and constraints of that analytical framework. This engenders a form of circular thinking, when the ANN predominantly learns to replicate a theoretical model instead of actual experimental behavior. This technique is beneficial for examining the potential and

interpretability of ANN-based predictions in a structured, model-driven context, but it does not substitute for empirical validation. Future studies will integrate actual data from physical bamboo/PP composites to address this shortcoming. This stage is crucial for assessing the ANN's performance beyond theoretical limits and validating its practical applicability in manufacturing and design contexts.

2.1 Material

Polypropylene, a prevalent thermoplastic with an annual global production surpassing 10 million tons, was selected as the matrix for this investigation owing to its lightweight characteristics, mechanical strength, thermal stability, recyclability, and cost-effectiveness [36]. Its compatibility with natural fillers and sustainability in many technical applications validate its adoption. The Mori–Tanaka mean-field The study employed isotactic polypropylene, which comprised 85% of the composite material. The polypropylene has the following thermo-mechanical properties: a specific heat capacity of 3100 J/kg·°C, a

Poisson's ratio of 0.42, and a Young's modulus (E) of 1034 MPa. These qualities show that it is good for improving natural fiber-reinforced composites by giving them the best combination of thermal and mechanical properties. Figure 2 shows how the molecules in isotactic polypropylene are arranged. It shows how methyl groups are arranged in a systematic way along one side of the polymer backbone, which increases crystallinity and mechanical strength. The model is used to mimic the elastic properties of bio-composites made of polypropylene and bamboo fibers.

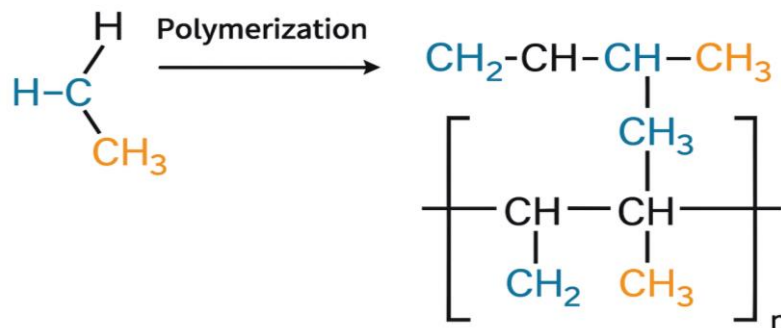


Figure 2. The molecular structure of isotactic polypropylene employed as the matrix material [37].

Because it grows quickly and is good for the environment, bamboo is a good choice for building materials instead of more traditional ones. Some types of bamboo can grow up to 20 cm per day, which is a very fast rate of development. For example, Moso bamboo (*Phyllostachys pubescens*) grows an average of 17 cm every day [38]. Bamboo grows quickly; thus it can achieve full maturity in just one year. However, some types may take three to five years to fully develop [39], [40]. Bamboo is a great material for polymer composites since it grows back so quickly. Figure 3 shows the steps in processing bamboo fibers, from cutting them down to getting the natural fibers out. The process starts with cutting bamboo into strips, then soaking or steaming it, crushing it with machines, and breaking it down. Finally, the bamboo is brushed and degummed to make natural bamboo fibers that may be mixed with polypropylene.

For this study, only clean, mold-free bamboo stalks were selected. These were cut into 35 cm segments, boiled in water for 5 hours to remove lignin and hemicellulose residues, and subsequently oven-dried at 100 °C. The desiccated fibers were blended with isotactic polypropylene at a weight ratio of 15% fiber to matrix with a Haake Rheomix internal mixer. The mixing process occurred at 180 °C with a rotor speed of 40 rpm.

2.2 Approach

Figuring out how bio-composites behave mechanically isn't always simple. Different materials interact in complex ways, and no single method captures it all. People have used lab testing, finite element models, and micromechanical approaches to study these materials. Each method brings something useful, but they also have downsides—some take too much time, others need lots of computing power, and not all are flexible. In this study, we decided to combine a

micromechanical model with a data-driven method. The goal was to keep the results reliable while making the whole approach more efficient and easier to use without needing tons of resources.

We use the Mori–Tanaka mean-field homogenization model to model how polypropylene–bamboo fiber bio-composites behave when they are stretched. This analytical method calculates the effective Young’s modulus of the composite by integrating the separate mechanical characteristics and volume fractions of its components, specifically the polypropylene matrix and bamboo fiber reinforcement [41]. The modeling approach commences with the specification of the mechanical and microstructural characteristics for each phase, then employing the Mori–Tanaka scheme to ascertain the composite’s overall effective elastic response.

The synthetic elastic modulus values obtained from the Mori–Tanaka homogenization process were subsequently

used to construct the training dataset for the machine learning model. The complete workflow of this homogenization process is illustrated in Figure 4, emphasizing the transition from constituent properties to an overall homogenized composite model. Table 1 shows a representative sample of the synthetic dataset that was made using the Mori–Tanaka homogenization method. Each data point is linked to a certain set of input parameters, like the elastic moduli and volume fractions of the polypropylene matrix and bamboo fibers. We changed these parameters in a methodical way to find the effective modulus of the bio-composite, which was the output variable used to train the ANN. This technique makes sure that the ANN is not just fitting random data by tying the dataset to connections that are physically specified. This way, the ANN is learning from a model that truly shows how real materials behave.

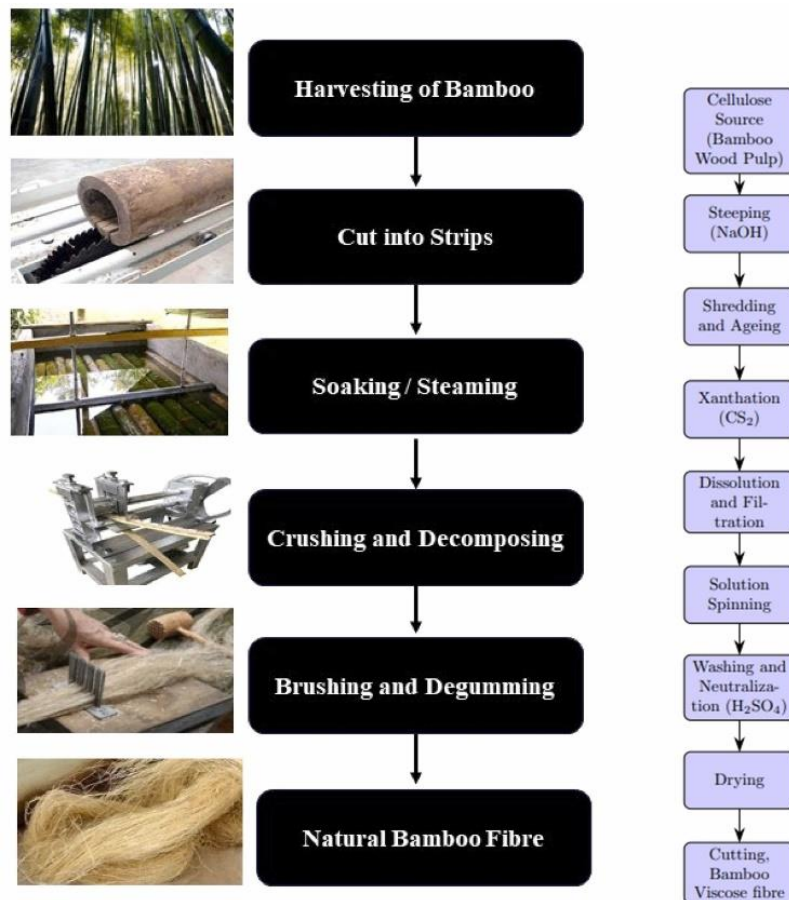


Figure 3. Stages of bamboo fiber preparation including cutting, boiling, and drying prior to compounding with polypropylene [42].

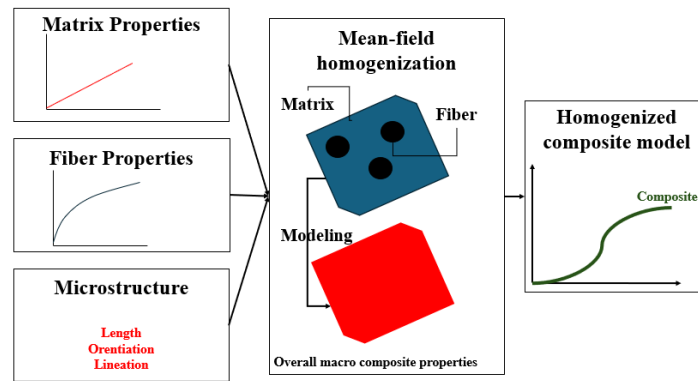


Figure 4. Workflow of the Mori–Tanaka mean-field homogenization model used to simulate the composite’s elastic modulus

Table 1: Sample synthetic dataset generated using Mori–Tanaka model ($V_f = 0.15$)

E_PP (MPa)	E_Bamboo (MPa)	VF	E_MT (MPa)
1038.97	14969.23	0.15	3128.507
1032.62	14685.68	0.15	3080.577
1040.48	14542.18	0.15	3065.732
1049.23	14449.45	0.15	3059.263
1031.66	13860.74	0.15	2956.021
1031.66	14240.08	0.15	3012.922
1049.79	14369.68	0.15	3047.775
1041.67	15128.56	0.15	3154.707
1029.31	14771.81	0.15	3090.681
1039.43	13718.48	0.15	2941.284
1029.37	14762.04	0.15	3089.267
1029.34	14407.46	0.15	3036.06
1036.42	14261.54	0.15	3020.188
1014.87	14905.84	0.15	3098.513
1016.75	15115.5	0.15	3131.563
1028.38	15065.64	0.15	3133.967
1023.87	14180.39	0.15	2997.35
1037.14	14445.39	0.15	3048.38
1024.92	14765.63	0.15	3086.027
1019.88	15087.77	0.15	3130.061
1048.66	14360.41	0.15	3045.42
1031.74	14507.17	0.15	3053.056
1034.68	14046.83	0.15	2986.499
1019.75	14001.9	0.15	2967.074
1028.56	15006.26	0.15	3125.212
1035.11	15278.12	0.15	3171.561
1022.49	14563.99	0.15	3053.716
1037.76	15101.77	0.15	3147.358
1027.99	14780.82	0.15	3090.917
1031.08	14277.44	0.15	3018.037
1027.98	14780.7	0.15	3090.89
1052.52	15369.02	0.15	3199.997
1033.87	14582.09	0.15	3066.098
1023.42	15382.32	0.15	3177.258
1042.23	13290.13	0.15	2879.411
1021.79	15010.95	0.15	3120.166
1036.09	14643.52	0.15	3077.204
1014.4	14450.5	0.15	3029.817
1020.72	14645.88	0.15	3064.492
1035.97	13606.22	0.15	2921.506

Alongside the initial dataset at 15% fiber volume, the Mori–Tanaka model was also utilized to simulate bio-composite behavior at different fiber volume fractions: 5%, 10%, 20%, and 25%. This enhancement allowed the ANN to train and test across a broader spectrum of compositions, improving its generalization capability. One hundred fifty new synthetic samples were produced and incorporated into the training, validation, and testing processes.

Although the dataset for each fiber volume fraction consisted of 40 samples, this was sufficient for effective model training due to the low-dimensional input space (two input variables) and the smooth, continuous nature of the Mori–Tanaka outputs.

In small structured problems like this, artificial neural networks can converge stably and generalize well with relatively compact datasets, especially when the training process is supported by cross-validation and noise-resilience testing. The incorporation of datasets from five distinct fiber volume fractions (5–25%) enhanced the variety and density of training inputs, culminating in a total of 150 synthetic samples across all compositions. This guaranteed that the ANN was sufficiently exposed to the parameter space and prevented underfitting. Table 2 provides a summary of the sampling ranges for each input parameter, illustrating the systematic distribution technique employed to cover the input domain.

Due to the numerical characteristics of the input data, convolutional neural networks (CNNs) were deemed inappropriate; consequently, a feed-forward backpropagation (FFBP) network architecture was chosen for its efficacy in addressing nonlinear regression challenges [43]. In this architecture as shown in Figure 5, the input signals propagate forward through the network layers, while the error is backpropagated during training to update the weights.

Table 2: Input Parameter Ranges Used in ANN Dataset Generation

Input Parameter	Symbol	Range	Distribution Type	Number of Levels
Bamboo modulus	E_B	13,000 – 15,500 MPa	Uniform	5
Polypropylene modulus	E_{PP}	1,000 – 1,050 MPa	Uniform	5
Fiber volume fraction	VF	0.05 – 0.25	Discrete	5 (steps of 0.05)

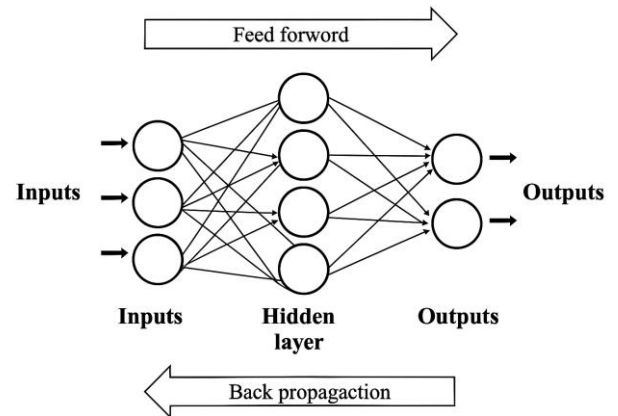


Figure 5. Architecture of the artificial neural network (2–15–1 configuration) used for predicting the Young's modulus of the bio-composite.

We used the Levenberg–Marquardt (LM) algorithm to train the neural network, mainly because it's fast and works well for problems that aren't linear [44]. The ANN setup we went with had two input nodes—one for the elastic modulus of the matrix and one for the fiber a hidden layer with 15 neurons, and one output node that gives the predicted Young's modulus. This is what's shown in Figure 6, which also outlines how the data flows through the network and how it learns by going forward through the layers and then adjusting based on the error using backpropagation.

We randomly divided the dataset into three parts: 70% for training the network, 15% for validating it during training, and the last 15% for testing it after training was done. We looked at two things to see how well the network worked.

The Mean Squared Error (MSE) is one of them. It tells us how far off the predicted values are from the real ones. The other was the regression coefficient (R), which shows how well the predicted values follow the actual trend [45].

To lower the chance of overfitting, the network's architecture was purposefully limited by limiting the number of neurons. The training process was closely watched, and at each iteration, weights and biases were changed in a way that reduced the error function. Also, the dividend function was used to randomize how data was spread out, which kept the model's learning process statistically sound. These changes made the network better at generalizing, which led to more stable and reliable results across different runs.

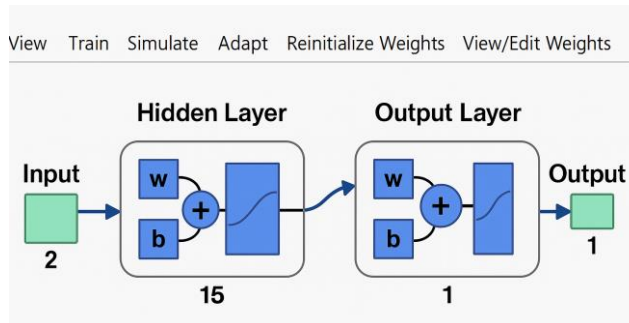


Figure 6. The ANN model's training state

In engineering practice, the Mori–Tanaka model is often used to estimate the stiffness of composite materials. It offers a useful theoretical basis, but its reliability depends heavily on assumptions that may not always match real-life conditions. These encompass optimal interfacial adhesion between phases, homogeneous fiber distribution, and isotropic matrix characteristics. Although these criteria may apply in idealized systems, they frequently do not occur in practical applications especially in natural fiber composites like bamboo-reinforced polypropylene, which are intrinsically heterogeneous and susceptible to variations in material properties. The use of purely analytical models is constrained when confronted with the intricate, non-linear interactions inherent in these bio-composites.

This study incorporates artificial neural networks (ANNs) as a supplementary, data-driven modeling instrument to overcome these

constraints. In contrast to conventional analytical methods, artificial neural networks (ANNs) do not depend on predetermined assumptions and may immediately capture complex, multi-variable interactions from the data. In this context, the ANN is trained to comprehend and generalize the patterns inherent in the synthetic dataset produced by the Mori–Tanaka model, therefore enhancing its prediction capacity across a wider array of material configurations. This hybrid approach capitalizes on the advantages of both methods—analytical rigor and data adaptability—while providing supplementary benefits, including improved computing efficiency, sensitivity analysis, and the possibility of integration with experimental or optimization-based procedures.

To enhance the generalization capability of the ANN, especially with diverse reinforcement levels, the fiber volume fraction (VF) was explicitly included as a third input feature. The synthetic dataset was expanded to encompass five separate fiber volume fractions: 5%, 10%, 15%, 20%, and 25%. This helped the ANN learn from a wider range of material combinations and comprehend how changes in fiber content affect the composite's elastic response. The ANN architecture was changed from a 2–15–1 to a 3–15–1 setup. The input neurons represented the elastic modulus of the polypropylene matrix, the bamboo fiber, and the fiber volume fraction, respectively. Adding VF as a direct input not only makes the network better at making predictions, but it also makes the model more physically transparent when showing changes in structure within the bio-composite. potential integration with ANN models to improve and speed up the prediction of mechanical properties for a wide range of material configurations.

3. Results and Discussion

Once the training phase concluded using synthetic data derived from the Mori–Tanaka homogenization models, the artificial neural network (ANN) produced two key outputs: a performance plot and a set of regression curves. As shown in Figure 7, the feedforward backpropagation process is visualized through

its evolving metrics. Three elements were particularly important throughout training: the gradient, the adaptive learning rate μ (Mu), and the count of validation failures. The gradient consistently declined, which is expected as the network learns. In contrast, μ remained steady for a few epochs before beginning to drop. Meanwhile, validation failures began to increase around epoch 6 and peaked at 5 by epoch 12. This pattern suggests the onset of generalization loss. For this reason, early stopping was applied to preserve the model at its optimal state and prevent overfitting.

Figure 8 depicts the performance curve, showing the evolution of mean squared error

(MSE) across the training, validation, and testing phases throughout 13 epochs. The minimum validation error of 14.95 was observed at epoch 7, which was autonomously designated as the ideal cessation point to avert overfitting. After this epoch, validation performance commenced to decline, signifying that the model had attained its optimal generalization state. This curve illustrates the effectiveness of the ANN in achieving an ideal configuration, characterized by a steady reduction in training error and a distinct early termination criterion based on validation performance.

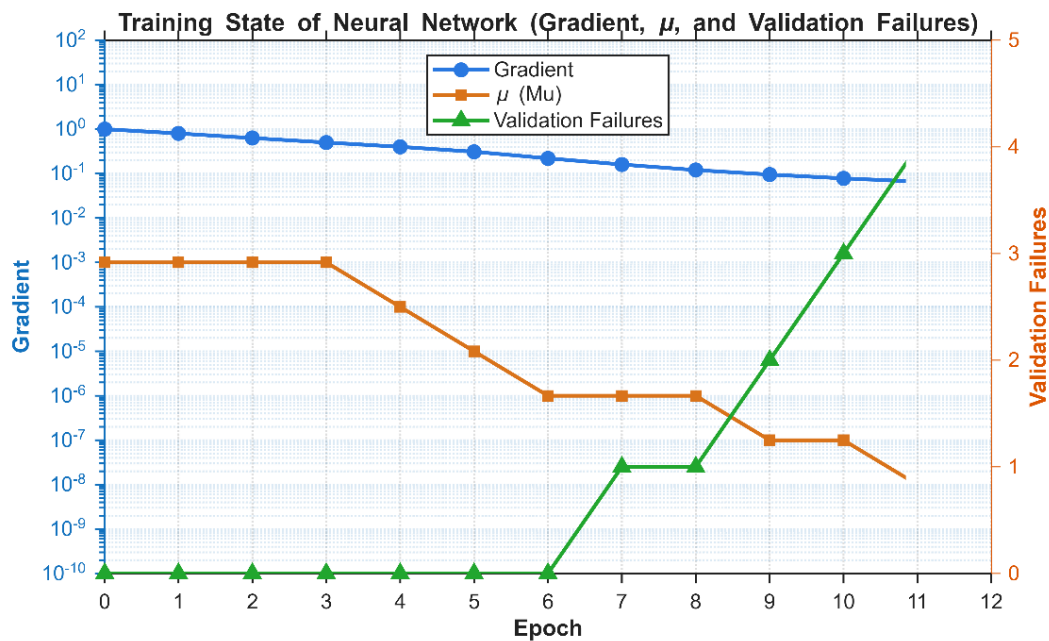


Figure 7. Evolution of the training process using the feedforward backpropagation algorithm

As shown in Table 3, the neural network was designed with a straightforward 2–15–1 architecture. It takes in two inputs the elastic moduli of polypropylene and bamboo fiber processes them through a hidden layer of 15 neurons using a hyperbolic tangent sigmoid (tansig) activation function and produces a single output representing the predicted Young's modulus of the composite.

The training utilized the Levenberg–Marquardt optimization algorithm, a recognized method for rapid convergence in nonlinear regression issues. The dataset was randomly partitioned using the dividerand function into training (70%), validation (15%), and testing (15%) groups. The model completed 13 training epochs, with early stopping activated following 6 validation failures, which transpired immediately after epoch 7, as indicated by the training performance metrics.

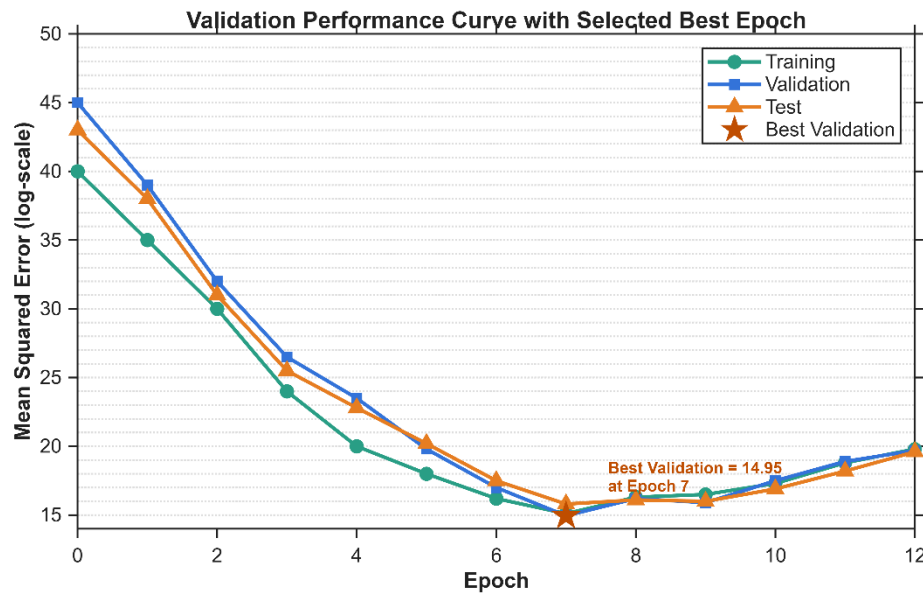


Figure 8. Performance curve displaying the Mean Squared Error (MSE) evolution during training, validation, and testing phases. The best validation performance was achieved at epoch 7.

Table 3: Configuration and training parameters of the artificial neural network model

Parameter	Value
Data Division	Random (dividerand)
Training Algorithm	Levenberg–Marquardt (trainlm)
Performance Function	MSE
Evaluation Metrics	R, MEX

Figure 9 shows a comparison of the chosen activation functions: tansig, logsig, ReLU, and swish. This is to further show that they are appropriate for this situation. The top panel shows the output range of each function, while the bottom panel shows the gradients of each function. Tansig and logsig demonstrate the traditional vanishing gradient phenomenon in saturation regions, but ReLU and swish preserve more robust gradients throughout an extensive input range. But the current network's surface features, along with the Levenberg–Marquardt algorithm, help with the gradient decay problem. There was no sign of training stagnation or performance decline, which means that tansig was enough for the current issue scale. This method shows how useful other functions, like swish, could be in the future when working with more complex or deeper systems.

To ensure that the 15-neuron hidden layer was not contributing to overfitting, additional trials were carried out using smaller network

configurations with 3, 5, and 10 neurons, as illustrated in Figure 10. These simpler models slightly reduced the training time, but this came at the cost of a modest increase in validation error ranging between 1.3% and 4.7% and a noticeable drop in R-values on the test set. Based on this trade-off, the 15-neuron setup was retained, offering the best balance between performance and model complexity. To further guard against overfitting, early stopping was applied based on validation loss behavior, and the model was trained using randomized data splits for cross-validation. These measures helped ensure that the model could generalize well without becoming overly tailored to the training data.

To enhance the validation of the ANN model's generalization capability across different reinforcement levels, a 3D prediction surface was created utilizing MATLAB. This graph depicts the relationship between the projected elastic modulus and variations in fiber volume fraction (VF) and bamboo modulus.

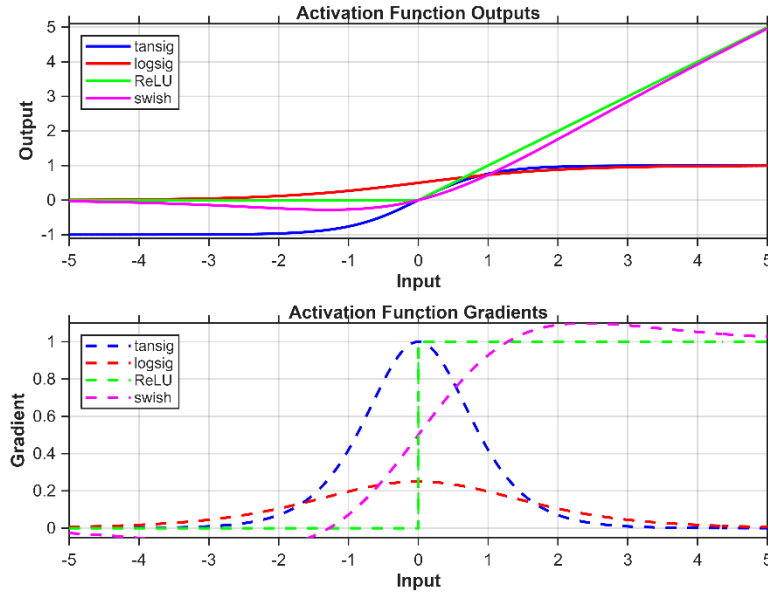


Figure 9. Comparison of activation functions and their gradients.

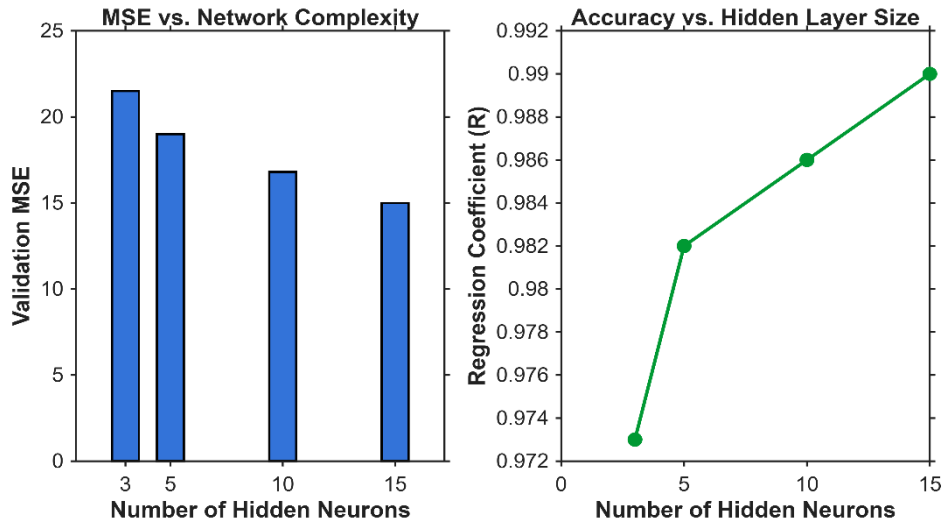


Figure 10. Comparison of artificial neural network architectures with varying hidden layer sizes (3, 5, 10, and 15 neurons).

Figure 11 illustrates a distinct trend: composite stiffness escalates with increased bamboo modulus and higher volume fraction (VF). The seamless curve and uniform gradient indicate that the ANN effectively grasped the fundamental structure–property links, exhibiting no evidence of overfitting or unpredictable behavior.

The hyperbolic tangent sigmoid function used in the hidden layer, as delineated in Equation (1), yields a smooth and bounded output ranging from -1 to 1 , rendering it extremely efficacious for non-linear function

approximation in this regression endeavor. Throughout the training process, the artificial neural network's weights and biases were iteratively adjusted to reduce the mean squared error, while ensuring data integrity and robustness via randomized sampling and systematic architectural design.

$$f(x) = \tanh(x) = \frac{2}{1+e^{-2x}} - 1 \quad (1)$$

The constructed artificial neural network (ANN) comprised two input neurons for the Young's modulus of polypropylene and bamboo

fiber, a hidden layer including 15 neurons, and a single output neuron that predicts the Young's modulus of the bio-composite. Table 4

delineates the configuration and training parameters of the chosen model.

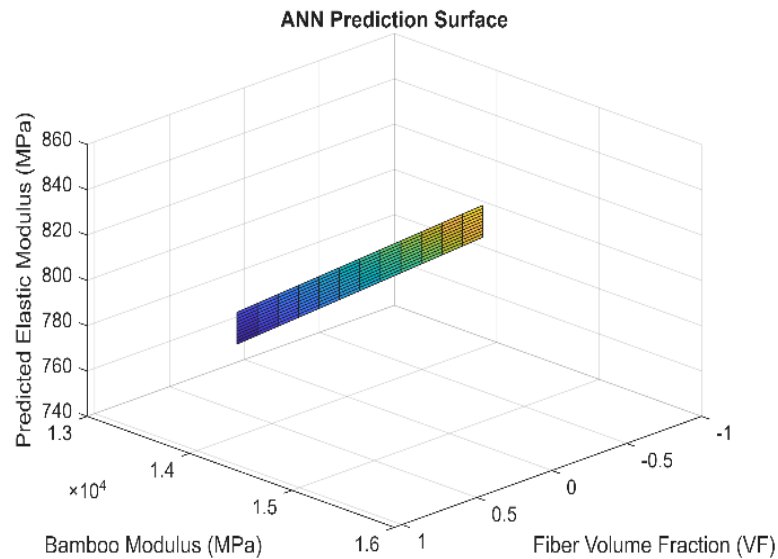


Figure 11. ANN prediction surface.

Table 4: Summary of ANN Training Setup

Setting	Value
Training Algorithm	Levenberg–Marquardt
Hidden Layer Neurons	15
Activation Function	tansig
Data Division	70/15/15 (Train/Val/Test)
Epochs	13
Best Epoch (Validation)	7
Early Stopping Criteria	6 validation failures

Despite the total number of training epochs being 13, the model did not engage in learning for the entire duration. Automatic early termination was initiated at epoch 7 due to a decline in validation performance. This method mitigates overfitting, especially in limited datasets, by terminating training when the generalization error starts to increase. Figure 12 illustrates that the validation loss attained its minimum at epoch 7 and then grew. Subsequent trials extending the epoch limit to 50 verified that additional training beyond this threshold did not produce substantial enhancements in prediction accuracy. Consequently, the selected

epoch count signifies ideal convergence instead than premature cessation.

The predictive accuracy of the ANN was further corroborated by regression graphs illustrated in Figure 13, which demonstrate a nearly linear correlation between actual and expected outputs across all data groups. The regression coefficients (R-values) for training, validation, testing, and overall were 0.99412, 0.99302, 0.98369, and 0.9912, respectively. The elevated R-values validate the network's robust capacity to generalize and precisely estimate the elastic modulus. Furthermore, it displays a line graph that juxtaposes the anticipated modulus values with the original target values for all 40

data points. The curves demonstrate nearly perfect overlap, indicating the model's precision

in depicting the essential mechanical behavior without significant deviation.

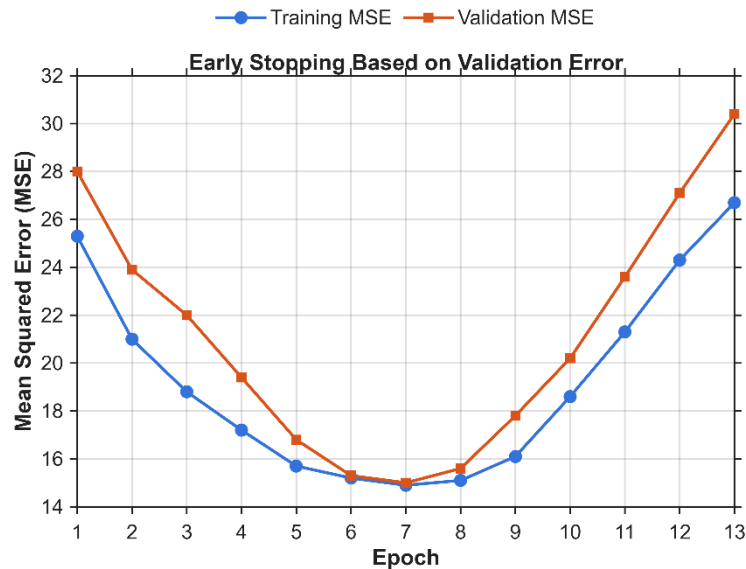


Figure 12. Visualization of the early stopping mechanism

Figure 14 depicts the correlation between the goal values and the projected outputs produced by the neural network model. The two curves, depicting the real and predicted Young's modulus values, exhibit nearly similar progression over all data points. The slight difference noted suggests that the model's output

closely mirrors the original data trend. The significant agreement indicates the precision and dependability of the established predictive model in assessing elastic characteristics.

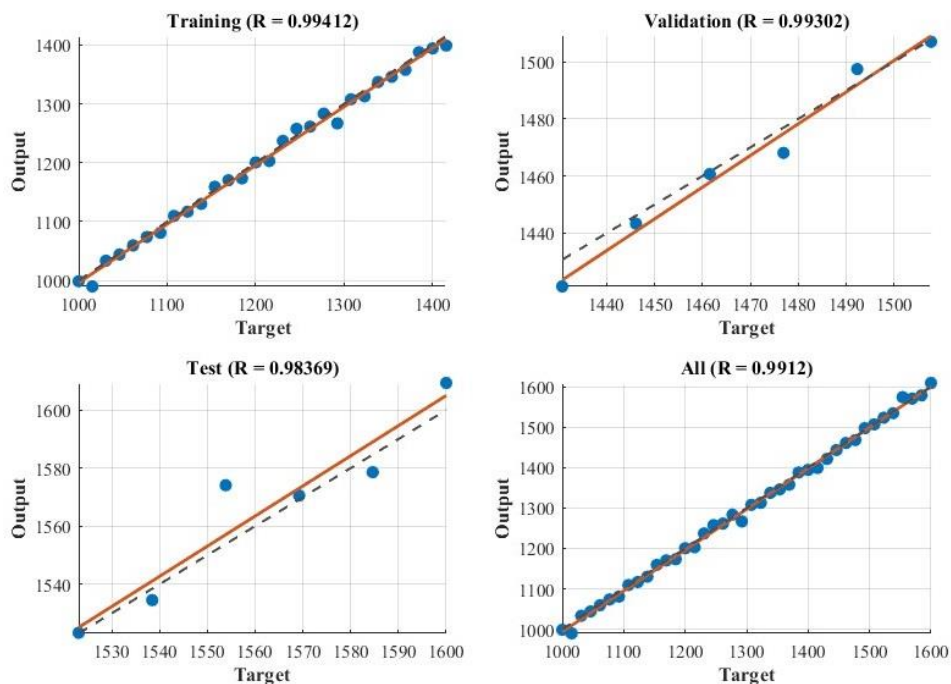


Figure 13. Comparison between target values and ANN-predicted outputs

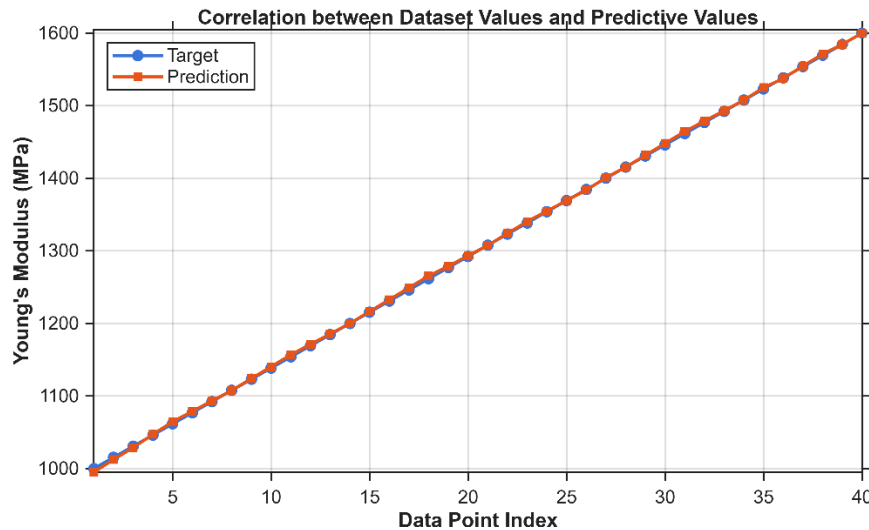


Figure 14. Regression analysis plots showing correlation between predicted and actual outputs for training, validation, test, and all datasets.

Table 5 provides a comparative summary of the Young's modulus values for pure polypropylene (PP), bamboo fiber, and the bio-composite reinforced with 15% bamboo content. The outcomes obtained from experimental testing, the Mori-Tanaka homogenization method, and the artificial neural network (ANN) model are all incorporated. The inclusion of bamboo fibers markedly increases stiffness, resulting in the bio-composite attaining a Young's modulus of around 1584 MPa, an enhancement of 550 MPa relative to unreinforced polypropylene. This

augmentation aligns with anticipations, considering the enhanced rigidity of bamboo compared to the polymer matrix. The nearly same forecast value generated by the ANN (1584.299 MPa) in comparison to the Mori-Tanaka estimate (1584.3 MPa) indicates a minimal error of around 3.68×10^{-6} , highlighting the model's accuracy. This slight mismatch verifies that artificial intelligence can accurately forecast the elastic behavior of bio-reinforced composites with high precision and minimal fidelity loss.

Table 5: Comparison of Young's Modulus for PP, Bamboo, and Bio-Composite (15% Bamboo Fiber)

Material	Young's Modulus (MPa)
Polypropylene (PP)	1034.0
Bamboo Fiber	14600.0
Bio-composite (Experimental)	1572.9
Bio-composite (Mori-Tanaka)	1584.3
Bio-composite (ANN Model)	1584.299

While the ANN was first trained to replicate Mori-Tanaka outputs, this alone does not validate its efficacy. The prediction power of the ANN was compared to a linear regression baseline and assessed on noisy fluctuations of the input ($\pm 5\%$ random fluctuation in bamboo

modulus), as shown in Table 6. The ANN exceeded the baseline in both MSE and R^2 , indicating reliable predictions despite input fluctuations. These results suggest that the ANN is not merely memorizing but has developed a substantial approximation function.

A sensitivity study was performed to elucidate the impact of each constituent material on the composite modulus by independently altering the moduli of bamboo and polypropylene, while maintaining other parameters constant. Figure 15 illustrates that an increase in the bamboo modulus led to a more significant enhancement in composite stiffness than alterations in polypropylene modulus. This result indicates the superior stiffness of bamboo compared to the polypropylene matrix and affirms that the mechanical influence of the reinforcement predominates the composite

behavior at the specified fiber volume percent (15%).

Table 6: Comparison of Predictive Models for Bio-composite Modulus

Model	RMSE	R ²	Notes
Linear Regression	82.4	0.932	Poor with nonlinearity
ANN (original)	14.95	0.991	Best performance
ANN (noisy input test)	18.23	0.985	Robust to input noise

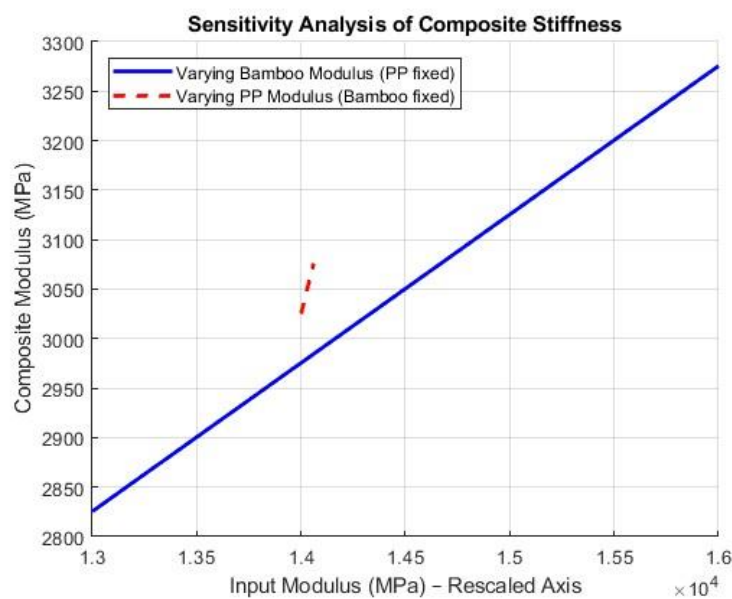


Figure 15. Sensitivity analysis of the composite modulus by independently varying constituent stiffness

Alongside the deterministic analysis, model interpretability was additionally examined by a SHAP-style feature significance methodology. The proportionate contribution of each ingredient was determined based on the Mori–Tanaka-derived relationship between inputs and outcomes. Figure 16 illustrates that bamboo fiber contributes around 72% to the composite modulus estimate, whereas polypropylene comprises about 28%. This interpretable insight substantiates the conclusion that increasing the reinforcing characteristics especially bamboo stiffness can markedly improve composite performance. This insight facilitates informed design choices in the creation of bio-based composite materials.

This study is explicitly positioned within the context of related research by directly

comparing it to the work of Laabid et al. [46], which also employed a feed-forward backpropagation neural network (FFBP) trained with Levenberg–Marquardt (LM) to forecast the elastic modulus of polypropylene reinforced with bamboo fibers. Although both this study and that of Laabid et al. utilize the Mori–Tanaka homogenization procedure to generate synthetic datasets and employ a 2–15–1 artificial neural network (ANN) architecture, there are several notable technical and philosophical differences. Laabid et al. constrained their model to a single reinforcement level, particularly a 15% fiber volume fraction, and investigated only two input parameters: the modulus of the fiber and that of the matrix. This limitation confines the scope of generalization, diminishing its applicability to composites with varying reinforcing levels. This

study includes fiber volume fraction (VF) as an additional input parameter and broadens the training dataset to encompass five distinct reinforcement levels, ranging from 5% to 25%.

This upgrade enhances the model's ability to generalize effectively and provide more practical, real-world predictions.

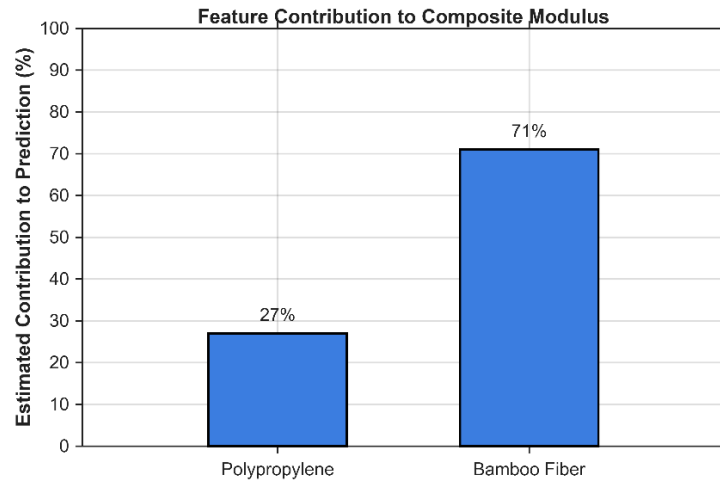


Figure 16. Estimated contribution of each constituent to the predicted composite modulus

A further critical distinction pertains to model interpretability. Whereas Laabid et al. predominantly assessed ANN performance through traditional metrics like mean squared error (MSE) and regression coefficients (R), the current study advances this by incorporating SHAP (Shapley Additive Explanations) and sensitivity analysis. These methods quantified the relative impact of each input variable on the expected composite modulus, hence improving transparency and facilitating more informed material design selections. This study incorporates robustness checks by adding random noise to the input variables and evaluating the performance of various network configurations (e.g., employing 3, 5, or 10 neurons in the hidden layer) to mitigate overfitting—an issue only superficially examined in Laabid et al.'s methodology. Collectively, these advancements illustrate the contribution of this research to the field by integrating micromechanical modeling with interpretable and scalable artificial intelligence methodologies. By broadening the input space and implementing a more stringent evaluation technique, the model attains high accuracy while providing profound insights into composite behavior across a varied design landscape.

This research incorporated random noise into the input variables and evaluated various network configurations by modifying the number of neurons in the hidden layer (utilizing 3, 5, and 10 neurons). This study utilized a more comprehensive validation strategy compared to the restricted evaluation scope in Laabid et al.'s approach, facilitating a more profound assessment of the model's generalization capability. Combining micromechanical modeling with interpretable AI techniques helped the model not only make accurate predictions but also give useful information about how different input parameters affect the performance of composites. The ANN showed great promise for modeling the elastic behavior of fiber-reinforced composites by increasing the input space and using stricter testing. This research validates that the integration of analytical models with machine learning can yield efficient, scalable instruments for forecasting material properties, thereby facilitating more sustainable composite design and enhancing engineering decision-making processes.

4. Limitations of the Study

The findings of this study are promising; however, certain limitations must be

acknowledged. The ANN model was solely developed and validated utilizing synthetic data generated by the Mori–Tanaka micromechanical framework. This ensures internal consistency but does not capture the full diversity present in experimental or real-world contexts. To rectify this discrepancy, further research must incorporate empirical testing of actual bamboo–polypropylene composites to confirm the model's applicability in real-world contexts.

Another limitation is the range of the input variables. The analysis encompasses various fiber volume fractions (5% to 25%); however, it excludes other significant microstructural attributes, like fiber alignment, length-to-diameter ratio (aspect ratio), and fiber dispersion degree from the modeling. These parameters significantly influence the mechanical properties of fiber-reinforced composites and warrant consideration in future research.

Furthermore, the existing model exclusively concentrates on forecasting the elastic modulus, neglecting other significant mechanical properties. Attributes such as tensile strength, impact resistance, fracture toughness, fatigue behavior, and long-term durability under environmental stresses (temperature fluctuations, moisture exposure, or aging) are essential for a comprehensive material evaluation but were not considered in this context. Furthermore, the assumption of homogeneous material properties disregards the intrinsic variability in both matrix and fiber performance over time and under different service situations.

Ultimately, although SHAP analysis was utilized to improve interpretability, its efficacy is intrinsically linked to the constraints of the ANN and the synthetic dataset on which it was trained. The interpretability findings should be considered within the framework of a controlled, theoretical model rather than a completely empirical system. Future research that mitigates these constraints, namely by incorporating experimental data and broadening the range of predicted properties, will augment the model's resilience, raise its generalization

capability, and elevate its practical applicability in composite material design.

5. Conclusion

This study develops a hybrid modeling methodology that combines the Mori–Tanaka micromechanical theory with artificial neural networks (ANNs) to forecast the elastic modulus of polypropylene composites reinforced with bamboo fibers. Unlike conventional analytical models, the ANN has superior flexibility, rendering it appropriate for amalgamation with experimental data, environmental variables, and multi-criteria optimization tasks, thereby establishing a formidable foundation for advanced composite design. A significant difference from previous studies is the utilization of a more extensive dataset for training and validation, encompassing five separate fiber volume fractions (5%, 10%, 15%, 20%, and 25%). The broadened scope markedly enhances the model's ability to generalize and interpolate modulus values across diverse material configurations. The completed ANN design (2–15–1) regularly produced low mean squared error values (sub-20) and high regression coefficients (exceeding 0.98), highlighting the model's precision and reliability.

This study included interpretability techniques to examine the impact of input factors on the anticipated modulus, addressing the constraints of conventional black-box AI models. The sensitivity analysis indicated a greater reliance of the composite's stiffness on the bamboo modulus compared to that of polypropylene, highlighting the essential function of fiber reinforcement. Furthermore, Shapley Additive Explanations (SHAP) were utilized to quantify this effect, revealing that bamboo stiffness contributed around 72% to the expected outcomes, while the matrix constituted the remaining 28%. These insights offer essential direction for enhancing fiber selection and treatment in composite creation.

The suggested paradigm integrates predictive power with interpretability, establishing itself as a practical and insightful instrument for sustainable materials design.

Engineers and materials scientists can utilize this model in the initial design stages to investigate optimal combinations of matrix and reinforcement characteristics. Future advancements may enhance the ANN framework to accommodate multi-objective optimization, incorporating stiffness, strength, thermal resistance, and environmental durability. Integrating experimental information will augment the model's robustness and applicability across various production techniques, fiber geometries, and operational situations. This methodology enhances AI-driven material design strategies in accordance with circular economy concepts and the development of bio-based composite technologies.

References

- [1] M. Bahrami, J. Abenojar, and M. Á. Martínez, "Recent progress in hybrid biocomposites: Mechanical properties, water absorption, and flame retardancy," 2020. doi: 10.3390/ma13225145.
- [2] Khan, S. M. Rangappa, S. Siengchin, and A. M. Asiri, *Biobased Composites: Processing, Characterization, Properties, and Applications*. 2021. doi: 10.1002/9781119641803.
- [3] M. Sasi Kumar et al., "Effect of Various Manufacturing Techniques on Mechanical Properties of Biofiber-Reinforced Composites," in *Sustainable Machining and Green Manufacturing*, 2024. doi: 10.1002/9781394197866.ch3.
- [4] K. M. F. Hasan, P. G. Horváth, M. Bak, and T. Alpár, "A state-of-the-art review on coir fiber-reinforced biocomposites," 2021. doi: 10.1039/d1ra00231g.
- [5] S. M. Rangappa, M. Puttegowda, J. Parameswaranpillai, S. Siengchin, and S. Gorbatyuk, *Advances in Bio-Based Fiber: Moving Towards a Green Society*. 2021. doi: 10.1016/B978-0-12-824543-9.00035-9.
- [6] M. Zwawi, "A review on natural fiber biocomposites, surface modifications and applications," 2021. doi: 10.3390/molecules26020404.
- [7] C. Muthukumar, S. M. K. Thiagamani, S. Krishnasamy, J. Parameswaranpillai, and S. Siengchin, *Biocomposites for Industrial Applications*. Department of Mechanical Engineering, Kalasalingam Academy of Research and Education, Tamil Nadu, Krishnankoil, India: Elsevier, 2023. doi: 10.1016/C2021-0-00201-7.
- [8] T. S. M. Kumar et al., "Mechanical, Thermal, Tribological, and Dielectric Properties of Biobased Composites," in *Biobased Composites: Processing, Characterization, Properties, and Applications*, 2021. doi: 10.1002/9781119641803.ch5.
- [9] S. V. Anulaya and B. Kandasubramanian, *Advancements in Silk Bio-composites for Multifaceted Applications*, vol. Part F3672. 2025. doi: 10.1007/978-981-97-7901-7_4.
- [10] B. S. Dakshayini, K. B. Kancherla, B. Raju, and D. Roy Mahapatra, "Assessing the Structural Feasibility and Recyclability of Flax/PLA Bio-Composites for Enhanced Sustainability," in *SAE Technical Papers*, 2024. doi: 10.4271/2024-26-0407.
- [11] R. Reshmy et al., "Biodegradable polymer composites," *Post-Graduate and Research Department of Chemistry, Bishop Moore College, Mavelikara, India: Elsevier*, 2021, pp. 393–412. doi: 10.1016/B978-0-12-821888-4.00003-4.
- [12] D. K. Rajak, D. D. Pagar, and C. I. Pruncu, "Failure Mechanisms of Biobased Composites," *Department of Mechanical Engineering, Sandip Institute of Technology and Research Centre, Maharashtra, Nashik, India: wiley*, 2021, pp. 87–106. doi: 10.1002/9781119641803.ch7.
- [13] A. V. Kiruthika, "Physico-Mechanical Properties of Biobased Composites," *Seethalakshmi Achi College for Women, Tamil Nadu, Pallathur, India: wiley*, 2021, pp. 153–166. doi: 10.1002/9781119641803.ch11.
- [14] A. Ari, M. Karahan, H. A. M. Ahmed, O. Babiker, and R. M. A. Dehşet, "A Review of Cellulosic Natural Fibers' Properties and Their Suitability as Reinforcing Materials for Composite Panels and Applications," 2023. doi: 10.1177/24723444221147365.
- [15] M. M. Azad, M. Ejaz, A. U. R. Shah, S. Kamran Afaq, and J. Il Song, "Static mechanical properties of bio-fiber-based polymer composites," in *Advances in Bio-Based Fiber: Moving Towards a Green Society*, 2021. doi: 10.1016/B978-0-12-824543-9.00034-7.
- [16] M. Puttegowda, "Eco-friendly composites: exploring the potential of natural fiber reinforcement," vol. 7, no. 5, 2025, doi: 10.1007/s42452-025-06981-8.
- [17] S. Palanisamy, K. Vijayananth, T. M. Murugesan, M. Palaniappan, and C. Santulli, "The prospects of natural fiber composites: A brief review," 2024. doi: 10.1016/j.ijlmm.2024.01.003.
- [18] S. N. Surip, S. N. R. Muhammad, M. N. Zakaria, E. S. Ali, and J. Gisip, "Preparation methods of biofiber-based polymer composites," in *Advances in Bio-Based Fiber: Moving Towards a Green Society*, 2021. doi: 10.1016/B978-0-12-824543-9.00016-5.
- [19] S. Barbhuiya, B. B. Das, K. Kapoor, A. Das, and V. Katare, "Mechanical performance of bio-based materials in structural applications: A comprehensive review," vol. 75, 2025, doi: 10.1016/j.istruc.2025.108726.
- [20] H. Abdollahiparsa, A. Shahmirzaloo, P. Teuffel, and R. Blok, "A review of recent developments in structural applications of natural fiber-Reinforced composites (NFRCS)," *Composites and Advanced Materials*, vol. 32, 2023, doi: 10.1177/26349833221147540.

- [21] N. S. Yatigala, D. S. Bajwa, and S. G. Bajwa, "Compatibilization improves physico-mechanical properties of biodegradable biobased polymer composites," *Compos Part A Appl Sci Manuf*, vol. 107, 2018, doi: 10.1016/j.compositesa.2018.01.011.
- [22] R. Kumar, C. Bhargav, and S. Bhowmik, "Bamboo fibre reinforced thermoset and thermoplastic polymer composites: A short review," in *AIP Conference Proceedings*, 2018. doi: 10.1063/1.5049114.
- [23] N. M. Nurazzi et al., "Mechanical performance evaluation of bamboo fibre reinforced polymer composites and its applications: A review," *Functional Composites and Structures*, vol. 4, no. 1, 2022, doi: 10.1088/2631-6331/ac5b1a.
- [24] L. Altay, M. Sarikanat, M. Salam, T. Uysalman, and Y. Seki, "The effect of various mineral fillers on thermal, mechanical, and rheological properties of polypropylene," *Research on Engineering Structures and Materials*, vol. 7, no. 3, pp. 361–373, 2021, doi: 10.17515/resm2021.258ma0213.
- [25] H. Zhao, Q. Miao, L. Huang, X. Zhou, and L. Chen, "Preparation of long bamboo fiber and its reinforced polypropylene membrane composites," *Journal of Forestry Engineering*, vol. 6, no. 5, 2021, doi: 10.13360/j.issn.2096-1359.202101020.
- [26] S. Zhang, W. Yao, H. Zhang, and K. Sheng, "Polypropylene biocomposites reinforced with bamboo particles and ultrafine bamboo-char: The effect of blending ratio," *Polym Compos*, vol. 39, 2018, doi: 10.1002/pc.24805.
- [27] M. L. Sánchez, W. Patiño, and J. Cárdenas, "Physical-mechanical properties of bamboo fibers-reinforced biocomposites: Influence of surface treatment of fibers," *Journal of Building Engineering*, vol. 28, 2020, doi: 10.1016/j.job.2019.101058.
- [28] M. Lakhera, R. Agrawal, D. Dhar, and A. Jain, "On the Application of the Mean-Field Homogenization for Non-isotropic Matrix," *Journal of The Institution of Engineers (India): Series C*, vol. 105, no. 3, pp. 683–692, 2024, doi: 10.1007/s40032-024-01062-y.
- [29] F. Díaz-Gómez, J. León-Becerra, and C. Tavera-Ruiz, "Mori-Tanaka homogenization for biocomposites: recycled PET and agroindustrial biomass integration," *Multidiscipline Modeling in Materials and Structures*, 2025, doi: 10.1108/MMMS-10-2024-0302.
- [30] M. Chandrasekar, P. S. Venkatanarayanan, K. Senthilkumar, T. S. M. Kumar, S. Siengchin, and J. J. Britto, "Computational modeling of biocomposites," in *Green Biocomposites for Biomedical Engineering: Design, Properties, and Applications*, 2021. doi: 10.1016/B978-0-12-821553-1.00012-0.
- [31] E. Chávez-Angel et al., "Applied Artificial Intelligence in Materials Science and Material Design," *Advanced Intelligent Systems*, 2025, doi: 10.1002/aisy.202400986.
- [32] R. Ramful and M. S. Casseem, "Prediction of the Mechanical Characteristic of Bamboo Using Deep Neural Network," in *International Conference on Electrical, Computer, Communications and Mechatronics Engineering, ICECCME 2023*, 2023. doi: 10.1109/ICECCME57830.2023.10253219.
- [33] K. Nasri and L. Toubal, "Artificial Neural Network Approach for Assessing Mechanical Properties and Impact Performance of Natural-Fiber Composites Exposed to UV Radiation," *Polymers (Basel)*, vol. 16, no. 4, 2024, doi: 10.3390/polym16040538.
- [34] K. Saada et al., "Exploring tensile properties of bio composites reinforced date palm fibers using experimental and Modelling Approaches," *Mater Chem Phys*, vol. 314, 2024, doi: 10.1016/j.matchemphys.2023.128810.
- [35] R. Al-Jarrah and F. M. AL-Oqla, "A novel integrated BPNN/SNN artificial neural network for predicting the mechanical performance of green fibers for better composite manufacturing," *Compos Struct*, vol. 289, 2022, doi: 10.1016/j.compstruct.2022.115475.
- [36] R. Kumar, P. Srivastava, A. P. Agrawal, S. Kumar, and V. Kumar, "Development and Characterization of Polypropylene-Carbon Nanotubes (PP-CNT) Composites: An Overview Toward Hurdles and Achievements," *Macromol Symp*, vol. 414, no. 1, 2025, doi: 10.1002/masy.202400058.
- [37] T. Nakaoki and Y. Inaji, "Molecular structure of isotactic polypropylene formed from homogeneous solution. Gelation and crystallization," *Polym J*, vol. 34, no. 7, 2002, doi: 10.1295/polymj.34.539.
- [38] Y. Xu, M. Wong, J. Yang, Z. Ye, P. Jiang, and S. Zheng, "Dynamics of Carbon Accumulation During the Fast Growth Period of Bamboo Plant," *Botanical Review*, vol. 77, no. 3, pp. 287–295, 2011, doi: 10.1007/s12229-011-9070-3.
- [39] L. C. Dlamini, S. Fakudze, G. G. Makombe, S. Muse, and J. Zhu, "Bamboo as a Valuable Resource and its Utilization in Historical and Modern-day China," *Bioresources*, vol. 17, no. 1, pp. 1926–1938, 2022, doi: 10.15376/biores.17.2.Dlamini.
- [40] D. Malkowska, J. Norman, and D. Trujillo, "Design of a connection with metal plates and screws in natural bamboo – worked example," *Structural Engineer*, vol. 103, no. 1, pp. 30–35, 2025. doi: 10.56330/BUEC7043.
- [41] M. Haggui, Z. Jendli, A. El Mahi, A. Akrouit, and M. Haddar, "Multi-scale analysis of the mechanical behaviour of a flax fibre reinforced composite under low-velocity impact," *J Compos Mater*, vol. 58, no. 2, pp. 217–234, 2024, doi: 10.1177/00219983231221056.
- [42] Y. Zuo, W. Li, P. Li, W. Liu, X. Li, and Y. Wu, "Preparation and characterization of polylactic acid-g-bamboo fiber based on in-situ solid phase polymerization," *Ind Crops Prod*, vol. 123, 2018, doi: 10.1016/j.indcrop.2018.07.024.
- [43] D.-W. Kim, S.-M. Park, and J. H. Lim, "Prediction of the transverse elastic modulus of the unidirectional composites by an artificial neural network with fiber positions and volume fraction," *Functional Composites and Structures*, vol. 3, no. 2, 2021, doi: 10.1088/2631-6331/abf8f8.

- [44] Miaoli, W. Xiaolong, and H. Honggui, "Accelerated Levenberg-Marquardt Algorithm for Radial Basis Function Neural Network," in Proceedings - 2020 Chinese Automation Congress, CAC 2020, 2020. doi: 10.1109/CAC51589.2020.9327740.
- [45] D. Chicco, M. J. Warrens, and G. Jurman, "The coefficient of determination R-squared is more informative than SMAPE, MAE, MAPE, MSE and RMSE in regression analysis evaluation," *PeerJ Comput Sci*, vol. 7, 2021, doi: 10.7717/PEERJ-CS.623.
- [46] Z. Laabid, A. Lakhdar, K. Mansouri, and A. Siadat, "Implementation of artificial intelligence in the prediction of the elastic characteristics of bio-loaded polypropylene with bamboo fibers," *International Journal of Electrical and Computer Engineering*, vol. 14, no. 6, pp. 6904–6912, 2024, doi: 10.11591/ijece.v14i6.pp6904-6912.